Molecular Therapy
Nucleic Acids
Original Article

Aptamer-mediated transcriptional gene silencing of *Foxp3* inhibits regulatory T cells and potentiates antitumor response

Andrea J. Manrique-Rincón,[1,2] Luciana P. Ruas,[1] Carolinne T. Fogagnolo,[1,6] Randall J. Brenneman,[3] Alexey Berezhnoy,[3] Bianca Castelucci,[1,4] Sílvio R. Consonni,[4] Eli Gilboa,[3] and Marcio C. Bajgelman[1,2,5]

[1]Brazilian Biosciences National Laboratory (LNBio), Brazilian Center for Research in Energy and Materials (CNPEM), Campinas 13083-100, Brazil; [2]Medical School, University of Campinas (UNICAMP), Campinas 13083-887, Brazil; [3]Department of Microbiology and Immunology, Dodson Interdisciplinary Immunotherapy Institute and Sylvester Comprehensive Cancer Center, University of Miami, Miller School of Medicine, Miami, FL 33136, USA; [4]Institute of Biology, University of Campinas (UNICAMP), Campinas 13083-862, Brazil; [5]Faculty of Pharmaceutical Sciences, University of Campinas, Campinas-SP 13083-871, Brazil; [6]Ribeirao Preto Medical School, Biomedical sciences, University of Sao Paulo, Sao Paulo-SP 14049-900, Brazil

The inhibition of immunosuppressive mechanisms may switch the balance between tolerance and surveillance, leading to an increase in antitumor activity. Regulatory T cells play an important role in the control of immunosuppression, exhibiting the unique property of inhibiting T cell proliferation. These cells migrate to tumor sites or may be generated at the tumor site itself from the conversion of lymphocytes exposed to tumor microenvironment signaling. Because of the high similarity between regulatory T cells and other lymphocytes, the available approaches to inhibit this population are nonspecific and may antagonize antitumor response. In this work we explore a new strategy for inhibition of regulatory T cells based on the use of a chimeric aptamer targeting a marker of immune activation harboring a small antisense RNA molecule for transcriptional gene silencing of *Foxp3*, which is essential for the control of the immunosuppressive phenotype. The silencing of *Foxp3* inhibits the immunosuppressive phenotype of regulatory T cells and potentiates the effect of the GVAX antitumor vaccine in immunocompetent animals challenged with syngeneic tumors. This novel approach highlights an alternative method to antagonize regulatory T cell function to augment antitumor immune responses.

INTRODUCTION

Regulatory T cells (Tregs) are a lymphocyte population that exhibit immunosuppressive ability and play an important role in homeostasis of the immune system.[1–3] Although Tregs confer protection tolerance against self-antigens, thereby protecting against autoimmune diseases, they also contribute to tumor-specific T cell tolerance, and their increased presence in tumor sites has been associated with poor clinical prognosis in several types of cancer.[4–8] There are two main subsets of Tregs: natural regulatory T cells (nTregs) that are generated in the thymus and induced regulatory T cells (iTregs), which develop from the conversion of naive CD4 T cells by microenvironment signaling.[9,10] Tregs are usually characterized by high expression of the interleukin-2 high-affinity receptor alpha chain (IL-2Rα) and the stable expression of transcription factor forkheadboxP3 (*Foxp3*).[11] The Fox*p*3 transcription factor is considered a master regulator of the immunosuppressive phenotype of Tregs.[12,13] Some mutations in *Foxp3* are associated with the development of autoimmune diseases; furthermore, the depletion of Tregs in the mouse model DEREG eradicates primary tumors and metastases.[14,15]

Fox*p*3 is a critical transcription factor for the development of functional Tregs and orchestrates the expression of >700 genes associated with control of the immunosuppressive phenotype of the Treg population.[16–19] The expression of *Foxp3* is a tightly regulated process, dependent on the promoter and key, conserved, noncoding sequences (CNSs) that serve as binding sites for a number of transcription factors.[17,20] Thus expression of *Foxp3* can be epigenetically controlled, repressed by methylation in some of these CNSs and in the promoter region.[21,22]

Several strategies have been used to inhibit Treg function for therapeutic gain in potentiating antitumor immune responses, such as depletion using monoclonal antibodies anti-CD25[23] and a CD25+ targeted system based on fusion protein-toxin conjugates.[23–25] The administration of metronomic cyclophosphamide is also reported as an inhibitor of CD4+CD25+ Tregs.[26] These strategies are not specific for Treg inhibition and can also antagonize the activity of other T cell populations. Therefore, Fox*p*3 can be considered a promising target in the inhibition of Tregs; however, because of its intranuclear location, it is necessary to develop strategies that allow vehiculation of efficient inhibitory molecules into the cell.

Received 17 July 2020; accepted 6 May 2021;
https://doi.org/10.1016/j.omtn.2021.05.005.

Correspondence: Marcio C. Bajgelman, Brazilian Biosciences National Laboratory (LNBio), Brazilian Center for Research in Energy and Materials (CNPEM), Campinas 13083-100, Brazil.
E-mail: marcio.bajgelman@lnbio.cnpem.br

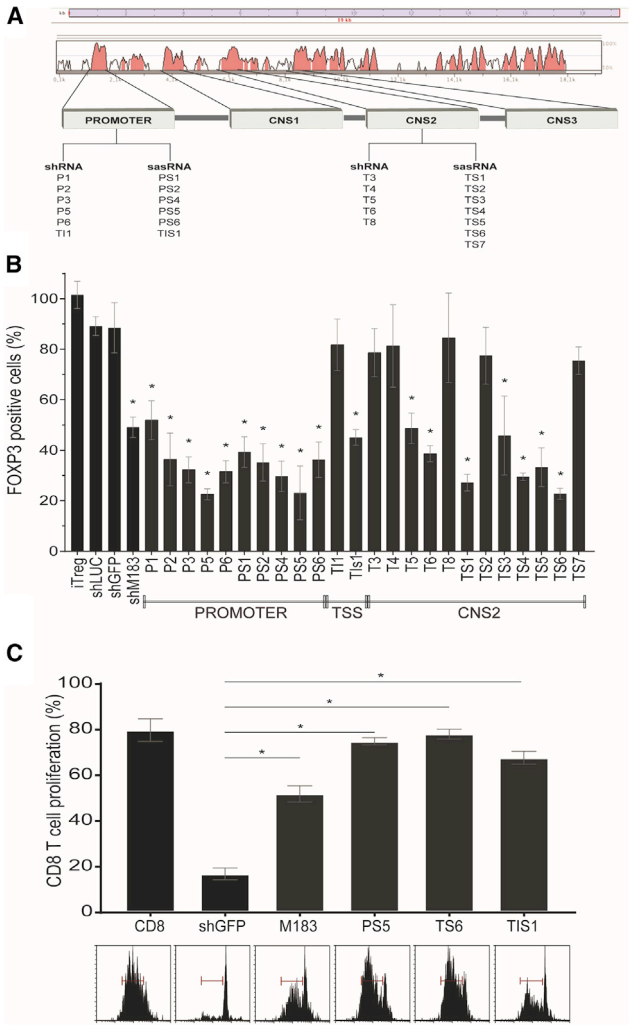

Figure 1. Silencing *Foxp3* with sasRNA candidates inactivates Treg immunosuppressive phenotype

(A) Schematic for RNAi candidate generation. Two sets of RNAi candidates were generated. In the first set we had shRNA candidates and in the second set the sasRNA candidates. All the RNAi candidates were designed to target specific sequences in the promoter region, transcriptional start site, or TSDR enhancer (CNS2), as indicated. (B) Flow cytometry assay to verify Fox*p*3 inhibition mediated by RNAi-lentivectors. iTregs were generated from primary CD4 T cells as described in Materials and methods and transduced with the indicated RNAi-lentivectors and incubated for 72 h. Cells were harvested, and Fox*p*3 expression was analyzed by permeabilizing cells and staining for FoxP3 by flow cytometry. (C) Silencing *Foxp3* is associated to inhibition of Tregs. T CD8 cells were CFSE labeled and incubated with iTregs transduced with RNAi-lentivectors as indicated. Below the graph bar are proliferation histograms of CFSE-labeled CD8 T cells. CD8, CD8 T cells without iTregs; shGFP, CD8 co-cultured with iTregs transduced with irrelevant RNAi lentivector; shM183, posttranscriptional RNAi candidate for FoxP3 inhibition. PS5, TS6, and TiS1 are TGS-RNAi-lentivectors. Graphs show mean and SEM. ANOVA and Dunnett's multiple comparison test (*$p < 0.05$). Results from three independent experiments performed in triplicate.

Here we propose utilization of transcriptional gene silencing (TGS) to inhibit *Foxp3*. In contrast to posttranscriptional gene silencing (PTGS) that consists of inhibiting mRNA, TGS is driven to the promoter or enhancer regions and may be associated with DNA methylation.[27–30] Our strategy is based on the generation of chimeric aptamers targeting cell surface proteins that can be used to vehiculate a small antisense RNA (sasRNA) to target cells via receptor-mediated endocytosis to induce TGS into the cell. These aptamers are short RNA strands fused to sasRNA at the 3′ end. We have chosen a previously described 4-1BB aptamer[31,32] to vehiculate the sasRNA to Tregs that constitutively express the 4-1BB costimulatory receptor. We show that aptamer-sasRNA-mediated TGS of *Foxp3* promotes antitumor responses in combination with GVAX, a cell-based vaccine consisting of irradiated tumor cells expressing the granulocyte-macrophage colony-stimulating factor (GM-CSF),[33] in immunocompetent mice challenged with syngeneic tumors.

RESULTS

Designing RNAi candidates for *Foxp3* transcriptional gene silencing

The *Foxp3* gene has conserved regions upstream of the start codon that are associated with transcriptional control (Figure 1A). The first region is the promoter that harbors the TATA box and CAAT sequence and transcriptional start site. The second and third regions are the respectively named CNS1 and CNS2 located in the second intron, whereas the fourth region, CNS3, is located between exons 1 and 2. Besides being conserved among species, a common feature observed in these regions is the presence of a high amount of CpG islands, which may be prone to methylation (Figure 1A; Figure S1). We have chosen the promoter and CNS2, which is also known as Treg-specific demethylated region (TSDR), as targets for designed TGS-RNAi candidates. (Table S1).[34] We generated two subsets of RNAi. The first set is represented by short hairpin RNA (shRNA) sequences targeting the promoter region, transcriptional initiation start site, and the TSDR enhancer region. The second set harbors sasRNA candidates targeting the same regions.

Silencing *Foxp3* in regulatory T cells by lentivirus-mediated RNAi-TGS

The TGS can be achieved by sasRNA designed to bind to promoter and enhancer regions.[35] The sasRNA is a single-strand RNAi molecule that binds to the DNA to inhibit gene transcription. Once we generated our sasRNA vectors, we transferred RNAi expression cassettes to lentiviral vectors that can be used for primary T cell transduction. These lentivectors also harbor a second expression cassette encoding CD90.1. This cell surface marker allows for identification of transduced cells in the flow cytometry analysis. Lentiviral vectors were titrated and used to transduce mouse CD4+ T cells in the presence of a Treg induction cocktail. When exposed to the induction cocktail, primary T cells should be converted to inducible Tregs (iTregs). In this way, our goal was to verify whether sasRNA vehiculated to primary T cells could prevent generation of iTregs, characterized by *Foxp3* expression. As shown in Figure 1B, several candidates of TGS-sasRNA inhibited *Foxp3* expression relative to control cassettes to luciferase or green fluorescent protein (GFP), and this inhibition was comparatively stronger than using a PTGS shRNA candidate named shM183.

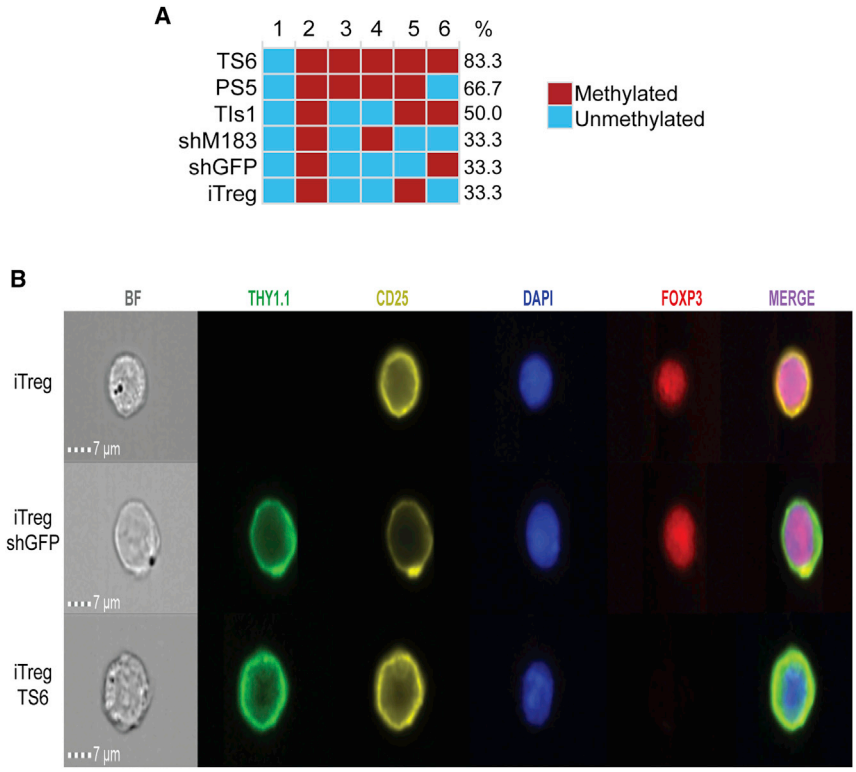

Figure 2. DNA methylation is increased in the promoter of *Foxp3* in TGS-RNAi transduced iTregs

(A) Representative diagram of CpG methylation on the promoter of iTregs that were transduced by lentiviral vectors. The CpG-rich hotspots are identified as 1, 2, 3, 4, 5, and 6. Blue squares represent unmethylated regions; red squares represent methylated regions (B) ImageStream analysis of iTregs stained with Thy1.1, CD25, DAPI (nuclear stain), and Foxp3. Representative images show nuclear localization of Foxp3 protein on cells transduced with the TGS candidate (TS6), shGFP, and a nontransduced cell (iTreg). Results from two independent experiments.

Next, we performed a proliferation assay to verify whether *Foxp3* silencing was associated with inhibition of immunosuppressive phenotype of Treg. Freshly isolated CD8 T cells were isolated from spleens of C57BL/6 mice and stained with carboxyfluorescein succinimidyl ester (CFSE). These CFSE-labeled cells were then incubated with iTreg-transduced cells and analyzed by flow cytometry (Figure 1C). Besides transducing iTregs with TGS-RNAi lentiviruses harboring candidates PS5 and TS6, we also transduced iTregs with the PTGS-RNAi candidate shM183 and control vectors encoding a non-endogenous-targeting shRNA sequence (shGFP) targeting GFP. We observed that TGS-RNAi lentivectors PS5 and TS6 show a significant rescue of CD8 proliferation, which was inhibited when iTregs were transduced with the negative control lentivector harboring shRNA-GFP (Figure 1C).

Transcriptional gene silencing mediated by TGS-RNAi candidates was associated with enhanced methylation in the Foxp3 *gene locus upstream of the start codon*

The literature suggests that TGS in mammalian cells may be associated with methylation in transcriptional control regions of the target gene.[27–29] We performed an *in vitro* experiment to evaluate methylation induced by lentivirus harboring TGS-RNAi candidates. Since TGS-RNAi was encoded into a lentivector that also harbors a CD90.1 expression cassette and transduced cells express both CD90.1 and TGS-RNAi, we did fluorescence-activated cell sorting (FACS) to isolate CD90.1 transduced Tregs. The gDNA was isolated, converted with bisulfite treatment, and profiled for methylation patterns. We chose 6 CpG sites in the promoter region of *Foxp3*. We then compared methylation patterns among gDNAs isolated from cells transduced with RNAi candidates and controls.

As seen in Figure 2A, candidates TS6 and PS5, which are sasRNAs targeted to the TSDR enhancer and promoter region, respectively, are the best-ranked candidates, inducing an 83.3% and a 66.7% methylation score, respectively, as assessed by methylation at selected CpG sites. The candidate TIS1, which targets the transcriptional initiation site, induced 50% methylation, whereas all the controls, the PTGS-RNAi shM183, the negative control shRNA-GFP, and Mock controls, exhibit only 33% methylation. With ImageStream analysis we can observe a decrease of *FoxP3* in the nucleus of iTregs with the TS6 candidate compared to controls (Figure 2B; Figure S2)

Aptamer-sasRNA chimeras mediate targeted transcriptional gene silencing of Foxp3 in regulatory T cells

The lentiviral vectors are reliable gene transfer tools and allowed us to screen TGS-RNAi candidates for *Foxp3* silencing. Considering the perspective of *in vivo* application of TGS-RNAi, we explored chimeric aptamers to vehiculate the best sasRNA candidates for *Foxp3* silencing. The previously described 4-1BB aptamer binds with high selectivity to 4-1BB receptor of activated T cells[32] and allows vehiculation of siRNA molecules.[31] We observed that the 4-1BB aptamer has the ability to bind 4-1BB receptor and translocates to the cell nucleus (Figure S4). In this way, we generated chimeric oligonucleotides that harbored a targeting moiety consisting of the previously characterized RNA aptamer to murine CD137 (4-1BB)[32] with a sasRNA portion that was cotranscribed at the 3′ end downstream of a previously described UCCC linker[31] (Figure 3A). The best candidates previously screened with lentivectors were chosen to generate sasRNA-aptamers, tested for *in vitro* activity to silence *Foxp3* expression and also evaluated for inhibiting immunosuppressive phenotype of iTreg (Figure S3). The 4-1BB-TS6 aptamer candidate mediated a significant reduction in *FoxP3* expression (Figure 3B), which correlates to the inhibition of the immunosuppressive phenotype of Treg in a proliferation assay, as assessed by flow cytometry (Figure 3C). It was also

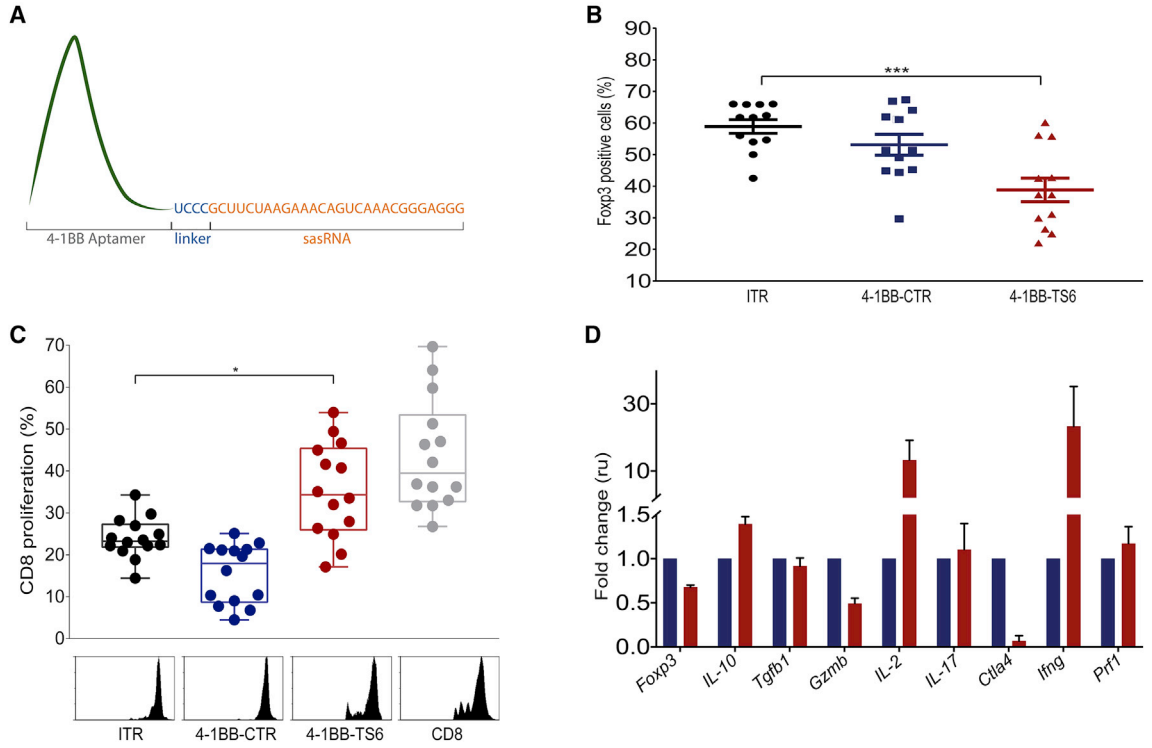

Figure 3. The aptamer 4-1BB-TS6 mediates *Foxp3* silencing and inhibits Treg immunosuppressive phenotype

(A) Representative figure for the 4-1BB sasRNA aptamer chimera. The sasRNA molecule is cotranscribed at the 3′ of the 4-1BB aptamer, separated by a 4 nucleotide UCCC linker. (B) Aptamer chimera TS6 inhibits FoxP3 expression in Tregs. iTregs were incubated with indicated aptamers at 500 nM; cells were stained for FoxP3 72 h after incubation and quantified by flow cytometry. (C) Aptamer chimera TS6 rescues the CFSE-labeled CD8 T cells from the inhibitory effects of iTregs. CD8 T cells were CFSE labeled and incubated with Tregs in the presence of indicated chimeras. iTreg, only inducible T regulatory cells; iTregs with 4-1BB-CTR, irrelevant aptamer; 4-1BB-TS6, sasRNA-aptamer chimera; CD8, only T CD8 cells. CD8 proliferation was assessed by dilution of CFSE. (D) 4-1BB-TS6 chimera induces alterations in gene expression of iTregs. iTregs were incubated with 4-1BB-TS6 aptamers (red bars) or control 4-1BB-CTR aptamer (blue bars). Cells were harvested 72 h after addition of 500 nM aptamer to isolate RNA. The cDNA was transcribed, and qPCR was performed. Gene expression was normalized by *Gapdh*. Graphs show mean and SEM. ANOVA and Dunnett's multiple comparison test (*$p < 0.05$). Results from three independent experiments.

investigated whether 4-1BB-sasRNA chimeras could alter iTreg gene expression. Aptamer chimeras to either 4-1BB-TS6 (which harbors the TGS RNAi for *Foxp3* silencing) or 4-1BB-CTR (a negative control aptamer) were incubated with iTreg *in vitro*. The cell culture was harvested after 72 h of incubation, and we performed a qPCR assay to profile gene expression for some targets that are known to be important for Treg phenotype and lymphocyte activation. We found enhanced *IL-2* and interferon gamma expression and also a decrease in *Ctla-4*, *Granzyme B*. and *FoxP3*. These changes are consistent with an inhibition of Treg immunosuppressive phenotype (Figure 3D)

Administration of 4-1BB-TS6 aptamer to tumor-challenged mice enhances antitumor response mediated by GVAX immunotherapy

To explore whether the chimeric aptamer 4-1BB-TS6 could improve the therapeutic benefit of an antitumor therapy, we performed *in vivo* experiments using immunocompetent mice challenged with syngeneic tumors primed with GVAX vaccination. Melanoma-derived B16F10 syngeneic cells were subcutaneously inoculated in C57BL/6 immunocompetent mice, and tumor growth was monitored. GVAX cells are genetically modified tumor cells that express GM-CSF and have been shown to promote antitumor immune responses.[33,36] The experimental outline can be seen in Figure 4A. Animals that received GVAX at days 1, 3, and 7 after tumor implantation show a reduction in tumor size, as previously demonstrated[36] (Figure 4B). Administration of 4-1BB-CTR with GVAX did not inhibit tumor growth more than GVAX alone. However, animals that received GVAX and 4-1BB-TS6 aptamer demonstrated a significant inhibition of tumor growth (Figure 4B).

DISCUSSION

The infiltration of Tregs in tumor sites represents one of the main immunosuppressive components in cancer immune tolerance.[7,37,38] A proposed mechanism for the FDA-approved checkpoint blockade inhibitor monoclonal antibody Yervoy (anti-CTLA-4) was to deplete Tregs, and although this is known to occur in mice, recent evidence from clinical samples indicates that this does not occur in the human tumor microenvironment.[39] Interventions that modulate Treg inhibition may be investigated to achieve better clinical outcomes. The Foxp3 transcription factor is considered the most specific marker of

Treg, and because of its role controlling the immunosuppressive phenotype it could be a molecular target for immunotherapy. However, given its intranuclear localization within Tregs, selective inhibition of *Foxp3* is challenging for antagonistic reagents. Here we demonstrated inhibition of Tregs *in vitro* and *in vivo* using sasRNA-based strategy for TGS, targeting two main noncoding regions of the *Foxp3* gene: the promoter region and the enhancer at the CNS2 region, also known as TSDR. Previous work from other groups has shown that shRNAs targeting a promoter sequence induce TGS in mammalian cells.[40,41]. Ackley et al. (2013) demonstrated that sasRNAs targeting the promoter are capable of TGS.[42] Besides the promoter region, expression of *Foxp3* also is driven by an enhancer region called TSDR. This TSDR is unmethylated in Tregs and methylated in conventional T cells. It is interesting to note that *Foxp3* expression can be modulated by methylation status, which is associated with immunosuppressive phenotype of this cell population.[43,44]

We hypothesized that TGS could be an efficient tool to downregulate *Foxp3* expression and inhibit immunosuppression mediated by Tregs. As seen in Figure 1, lentivectors harboring sasRNA targeted to the *FoxP3* promoter or TSDR could silence *Foxp3* and impaired Treg immunosuppressive phenotype (Figure 1C). In addition to *Foxp3* silencing and immunosuppression impairment, a qPCR assay for gene expression profiling also revealed some alterations that could be associated with an "ex-Treg" phenotype.[45,46] These are related to an increased expression of *IL-2* and interferon gamma and a decreased expression of *Ctla4* and Gzmb Granzyme B. However, these cells still conserve expression of *IL-10* and transforming growth factor β (TGF-β)[47] (Figure 3D).

The TGS is an attractive approach to regulate gene expression. In contrast to PTGS that needs a constant supply of RNAi molecules to inhibit target mRNA, TGS requires one molecule that acts at DNA and inhibits RNA transcription, silencing gene expression. Therefore the TGS system may employ fewer RNAi molecules that can be vehiculated by aptamer vectors. In this manner, chimeric RNAi-aptamers may be explored as transfer tools, because of their selectivity for target cells and ability to deliver the RNAi cargo.[30,31,48] Aptamers are chemically synthesized molecules that can be employed for systemic delivery of therapeutics because of their specificity, short half-life *in vivo*, and reduced immunogenicity.[49,50] In this work we explored the utilization of chimeric sasRNA-aptamer candidates that bind to the costimulatory cell surface receptor 4-1BB expressed on activated T cells[51] and may be internalized in the target cells to inhibit *Foxp3* transcription factor. The 4-1BB aptamer was engineered to harbor a *Foxp3*-silencing sasRNA molecule at 3′ extension, in one unique molecule. The chimeric TGS-aptamer is internalized through the 4-1BB cell surface receptor, translocates to the cell nucleus (Figure S4), and inhibits *de novo* transcription of *Foxp3* (Figure S5). We investigated whether a sasRNA targeting strategy using a murine 4-1BB aptamer had therapeutic effect in the poorly immunogenic syngeneic tumor challenge model of B16F10 cells on C57BL/6 mice. In our experiments an additive antitumoral effect *in vivo* was observed when using the aptamer 4-1BB-TS6 in coadministration with the GVAX immunotherapy (Figure 4). Data in the literature also have shown other therapeutic approaches that explore enhancement of antitumor response combining checkpoint inhibitors such as anti-PD1 or anti-CTLA4 with Treg inhibition, which suggests the potential of this strategy.[52,53] The approach using sasRNA-aptamer has two levels of selectivity: (1) targeting of 4-1BB-positive cells with a monomeric form of the 4-1BB aptamer and (2) delivery of a sasRNA targeting FoxP3, which is a transcription factor with limited expression/function in non-Treg cells. Since *Foxp3* silencing inhibits immunosuppressive activity of Tregs, this therapeutic approach should be harmless to cytotoxic CD8 T cells and activated CD4 T cells, and may even prevent generation of iTregs in the tumor site. The attenuation of Treg function is a proven immunotherapeutic strategy in preclinical models, which may have benefit for clinical translation.[7,37]

In conclusion, we developed a new tool for immunotherapy based on sasRNA-aptamers to induce a targeted TGS of *Foxp3* in Tregs. These chimeric aptamers inhibited the immunosuppressive phenotype of Tregs and potentiated GVAX antitumor immunotherapy. It is plausible that sasRNA targeting of other immunosuppressive receptors such as PD-1 or CTLA-4 or cytokine receptors such as TGF-β receptor II in CD8 T cells may be a means to transiently or permanently induce epigenetic changes that could augment antitumor immune responses. The strategy described here may present a novel approach to cancer immunotherapy through aptamer-targeted epigenetic modulation.

MATERIALS AND METHODS

Design and cloning of RNAi candidates targeting *Foxp3*

The TGS-RNAi candidates were chosen from regions of high homology between mouse and human sequences (NCBI accession numbers AF277994.1 for murine *Foxp3* and NG_007392.1 for human FOXP3) that share a high frequency of CpG sites. rVista[54] software was used to select candidates in the hotspot regions of *Foxp3*, as previously described by Ackley et al. (2013),[42] using an algorithm kindly provided by Dr. Kevin Morris, University of New South Wales, Australia. The shRNA candidates were generated by HPC dispatcher (City of Hope Bioinformatics Core, Duarte, CA, USA).[55]

The RNAi candidates with high affinity for the chosen regions were analyzed by BLAT[56] and checked for low predicted off-target effects. The oligonucleotide sequences for candidate sasRNAs and shRNAs were synthesized (IDT, USA) flanked by cohesive ends and cloned in the PLKO vector THY1.1 using BamHI and EcoRI (Table S1).

Viral production and titration

Viral vectors were generated from a pLKO backbone with the reporter CD90.1. Oligonucleotides harboring RNAi sequences were cloned at BamHI and EcoRI sites. Lentiviral vector production and titration were performed by the Viral Vector Laboratory at LNBIO, CNPEM, as previously described.[57]

Aptamer generation

DNA aptamer templates were amplified by standard PCR using the oligonucleotide sequences described in Table S1. PCR products were

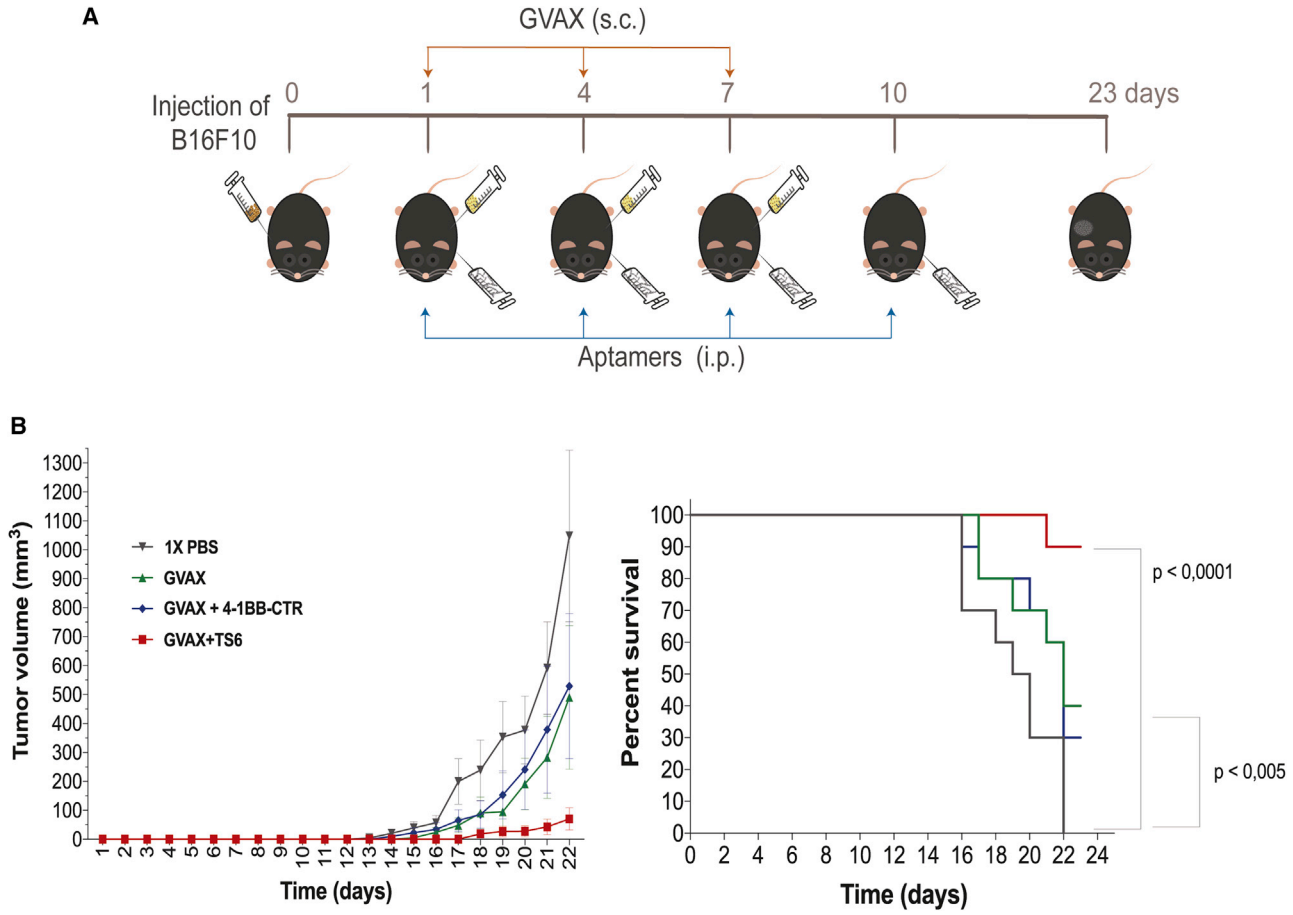

Figure 4. The 4-1BB-TS6 enhance antitumor response when combined with GVAX immunotherapy

(A) Experimental design for *in vivo* experiment. Animals were implanted with B16F10 cells in the right flank on day 0. GVAX was administered via subcutaneous injection on days 1, 4, and 7 and aptamers via i.p. injection on days 1, 4, 7, and 10. Animals were euthanized when tumor growth of PBS group had reached 1,000 mm^3. (B) Tumor growth and Kaplan-Meier survival curves in C57BL/6 mice bearing subcutaneous B16F10 tumors treated with aptamers and GVAX (n = 10 mice per group). The log-rank Mantel-Cox test was used to compare survival curves.

purified using QIAprep spin columns (QIAGEN). RNA aptamers were transcribed with the DuraScribe T7 Transcription Kit (Epicentre). The products were purified by 10% polyacrylamide gel electrophoresis and concentrated on a 30 kDa Amicon Ultra-4 column (Millipore, Billerica, MA, USA) in TE buffer (10 mM Tris-HCl (pH 8.0) 0.1 mM EDTA). We performed *in silico* prediction of aptamer structure with RNAstructure software[58] (Figure S6).

Approval of the ethics and biosafety committees

This study was approved by the Commission for Ethics in the Use of Animals of UNICAMP (protocol no. 2661-1) and the Internal Commission of Biosafety of CNPEM (file no. MCB3-090114).

Immunomagnetic isolation of primary CD4 and CD8 T cells

Isolation of CD4 and CD8 was performed from spleens of 8- to 12-week-old C57BL/6 male mice. Splenocyte preparations were generated by surgical isolation of spleens from sacrificed mice, and single-cell preparations were prepared with 70-μm mesh. CD4 or CD8 T cell preparations were generated with the EasySep CD4/CD8 T cell negative selection enrichment kit (StemCell, USA). The efficiency of these isolations was routinely higher than 90% as assessed by flow cytometry using antibodies for CD4 and CD8.

In vitro assay to evaluate *Foxp3* inhibition

Briefly, CD4+ T cells were activated for 24 h with plate-bound anti-CD3e (TONBO Biosciences clone 145-2C11) and CD28 (TONBO Biosciences clone 37.51) at a concentration of 1 μg/mL. The cells were cultured in a complete RPMI (CM) medium (1% penicillin-streptomycin, 1% HEPES, 1% sodium pyruvate, 1% nonessential amino acids, 1% glutamine, 10% fetal bovine serum [FBS], and 50 μM β-mercaptoethanol). Concentrated virus preparations encoding RNAi candidates or controls were used to transduce CD4+ T cells using a multiplicity of infection (MOI) of 10. The vectors were incubated with 8 mg/mL polybrene, IL2 100 U/mL, TGFβ 1 ng/mL, and retinoic acid 100 nM for 24 h; then the medium was replaced with fresh CM medium containing IL2 100 U/mL, TGFβ 1 ng/mL, and

retinoic acid 100 nM. Cells were then incubated for 72 h and harvested for flow cytometry.

Flow cytometry of Foxp3

Cells were initially labeled with anti-CD90.1 (thy1.1)-fluorescein isothiocyanate (FITC) (eBioscience, USA) and anti-FOXP3-allophycocyanin (APC) (eBioscience, USA), following the instructions from the manufacturer. Cells were resuspended in 1× PBS and analyzed by flow cytometry. *Foxp3* expression was evaluated from CD90.1 gated cells. The samples were analyzed on the FACSCanto II flow cytometer (BD Biosciences, USA), and data analysis was performed with FCS Express 5 Research Edition.

ImageStream analysis

Data acquisition was performed on an imaging flow cytometer (ImageStreamX; Amnis/EMD Millipore, Seattle, WA, USA). Image analysis was performed with IDEAS 6.2 software. Mean similarity was calculated using Pearson's correlation coefficient. Cells within the gate R2 have a similarity $\geq$ 1 between DAPI and Foxp3, indicating nuclear Foxp3 (Figure S2).

Immunosuppression assay using Tregs treated with TGS candidates and effector CD8 cells

Spleens from C57BL/6 mice were dissociated and treated with ammonium-chloride-potassium (ACK) to do the lysis of red blood cells for 5 min at 4°C, and after washing with 1× PBS, 1×10^7 cells were incubated with 1 mg/mL of Mitomycin C (Sigma, USA) for 45 min at 37°C (these cells are referred to as APCs). The remainder of the splenocytes were used to separate CD8-positive cells by negative selection as described, and purity was assessed by CD8+ flow cytometry. CD8+ T cells were then labeled with CFSE (Thermo, USA) (1 μM). Tregs were transduced with RNAi viral vectors, using MOI = 10, in DMEM 10% FBS, supplemented with 8 μg/mL of polybrene or incubated with 500 nM of TGS-Aptamers in DMEM 10% FBS. CFSE-labeled CD8+ cells stained with CFSE and the APCs were plated with anti-CD3e antibody (clone 145-2C11, TONBO Biosciences, USA) at 0.5 μg/mL. After 72 h the cells were labeled with anti-CD8-PE (TONBO Biosciences, USA) and the proliferation of CD8 cells was assessed by the CFSE profile. CD8-PE labeling allows the exclusion of Tregs from the analysis.

Methylation analysis

Target cells were sorted based on the virus reporter CD90.1 expression after the *in vitro* assay to evaluate *Foxp3* inhibition. DNA was isolated and converted with bisulfite treatment using the EpiTech Kit (-QIAGEN, USA). After conversion, the promoter was amplified by PCR; this product was purified and sequenced. The methylation analyses were done with the Bisulfite sequencing DNA Methylation Analysis (BISMA) tool.[59] Oligonucleotide primers are listed in Table S1.

Real-time quantitative PCR

The RNA was isolated with the RNAeasy Kit (QIAGEN, USA) following reverse transcription to cDNA using a high-capacity cDNA transcription kit (QIAGEN, USA). The resulting cDNA libraries from each sample were then analyzed by qPCR for the genes *Foxp3*, *IL-2*, *IL-10*, *IL-17*, *Tgfβ*, *Gzmb*, *Prf1*, *Ctla4*, and interferon gamma. Gapdh was used as a housekeeping gene. The experiment was performed with 7500 v 2.6 software (Applied Biosystems, USA). Oligonucleotide primers are listed in Table S1.

Animal studies

The animals used in this work were 6- to 8-week-old male C57BL/6 mice. All animals were kept in microisolators and treated according to the animal care regulations of the CNPEM laboratory in the LNBIO-CNPEM animal facility. Mice (n = 10 per group) were injected into the right flank s.c. with 5×10^4 B16F10 cells in 100 μL of PBS, then treated on days 1, 4, and 7 post-implantation with 1×10^6 irradiated B16F10-GVAX cells (50 Gy) on the left flank of the animals and intraperitoneal (i.p.) injection of aptamers (250 pmol). On day 10 mice received a last injection of aptamers without vaccine (n = 10). Percent survival was expressed as percentage of mice without tumor among total injected mice, and tumor size was measured with a pachymeter and calculated as the longest diameter × smallest diameter × diagonal diameter divided by 3.141599/2 (in cubic millimeters).

Statistical analysis

Data were analyzed with Prism 7.0 (GraphPad). The experiments were repeated as indicated in the figure legends. Statistical significance was determined by unidirectional ANOVA and Dunnett's multiple comparison test. Tumor survival data were analyzed with the Kaplan-Meier method. The Mantel-Cox log-rank test was used to compare survival curves for different groups (*$p \leq 0.05$, **$p \leq 0.005$, ***$p \leq 0.001$).

SUPPLEMENTAL INFORMATION

Supplemental information can be found online at https://doi.org/10.1016/j.omtn.2021.05.005.

ACKNOWLEDGMENTS

We thank the Viral Vector lab and the animal facility at LNBio-CNPEM for providing the viral vector preparations and animal care, as well as Eugenia Camargo for assistance with flow cytometry. We also thank the Flow cytometry facility at UNICAMP for assistance with cell-sorting and AMNIS experiments. We thank the hematology core at UNICAMP for cell irradiation for GVAX generation and Michel Vaz de Oliveira for helping with animal experiments. We thank Dr. Glenn Dranoff for kindly providing GM-CSF B16F10 cells, Dr. Kevin Morris for support with the transcriptional gene silencing algorithm, as well as Dr. Andrew Waters for his careful reading and helpful comments on the manuscript. This work was supported by Fundação de Amparo à Pesquisa do Estado de São Paulo (FAPESP) (Grants MCB-2012/13132-0 and MCB-2019/04458-8 and the fellowship AJMR-2013/02041-6).

AUTHOR CONTRIBUTIONS

A.J.M.-R. conceived and performed experiments, analyzed data, and wrote the manuscript. L.P.R., B.C., and C.T.F. performed

experiments. R.J.B. and A.B. provided expertise. S.R.C. provided expertise and performed experiments. E.G. provided expertise and discussed results. M.C.B. supervised the study, conceived experiments, analyzed data, wrote the manuscript, and provided funding.

DECLARATION OF INTERESTS

The authors declare no competing interests.

REFERENCES

1. Feuerer, M., Hill, J.A., Mathis, D., and Benoist, C. (2009). Foxp3+ regulatory T cells: differentiation, specification, subphenotypes. Nat. Immunol. *10*, 689–695.
2. Josefowicz, S.Z., Lu, L.F., and Rudensky, A.Y. (2012). Regulatory T cells: mechanisms of differentiation and function. Annu. Rev. Immunol. *30*, 531–564.
3. Han, S., Toker, A., Liu, Z.Q., and Ohashi, P.S. (2019). Turning the Tide Against Regulatory T Cells. Front. Oncol. *9*, 279.
4. Zhou, G., and Levitsky, H.I. (2007). Natural regulatory T cells and de novo-induced regulatory T cells contribute independently to tumor-specific tolerance. J. Immunol. *178*, 2155–2162.
5. Shang, B., Liu, Y., Jiang, S.J., and Liu, Y. (2015). Prognostic value of tumor-infiltrating FoxP3+ regulatory T cells in cancers: a systematic review and meta-analysis. Sci. Rep. *5*, 15179.
6. Betts, G., Jones, E., Junaid, S., El-Shanawany, T., Scurr, M., Mizen, P., Kumar, M., Jones, S., Rees, B., Williams, G., et al. (2012). Suppression of tumour-specific $CD4^+$ T cells by regulatory T cells is associated with progression of human colorectal cancer. Gut *61*, 1163–1171.
7. Ohue, Y., and Nishikawa, H. (2019). Regulatory T (Treg) cells in cancer: Can Treg cells be a new therapeutic target? Cancer Sci. *110*, 2080–2089.
8. D'Arena, G., Laurenti, L., Minervini, M.M., Deaglio, S., Bonello, L., De Martino, L., De Padua, L., Savino, L., Tarnani, M., De Feo, V., and Cascavilla, N. (2011). Regulatory T-cell number is increased in chronic lymphocytic leukemia patients and correlates with progressive disease. Leuk. Res. *35*, 363–368.
9. Hsieh, C.S., Lee, H.M., and Lio, C.W. (2012). Selection of regulatory T cells in the thymus. Nat. Rev. Immunol. *12*, 157–167.
10. Bilate, A.M., and Lafaille, J.J. (2012). Induced CD4+Foxp3+ regulatory T cells in immune tolerance. Annu. Rev. Immunol. *30*, 733–758.
11. Wing, K., and Sakaguchi, S. (2010). Regulatory T cells exert checks and balances on self tolerance and autoimmunity. Nat. Immunol. *11*, 7–13.
12. Fontenot, J.D., Gavin, M.A., and Rudensky, A.Y. (2003). Foxp3 programs the development and function of CD4+CD25+ regulatory T cells. Nat. Immunol. *4*, 330–336.
13. Hori, S., Nomura, T., and Sakaguchi, S. (2003). Control of regulatory T cell development by the transcription factor Foxp3. Science *299*, 1057–1061.
14. Brunkow, M.E., Jeffery, E.W., Hjerrild, K.A., Paeper, B., Clark, L.B., Yasayko, S.A., Wilkinson, J.E., Galas, D., Ziegler, S.F., and Ramsdell, F. (2001). Disruption of a new forkhead/winged-helix protein, scurfin, results in the fatal lymphoproliferative disorder of the scurfy mouse. Nat. Genet. *27*, 68–73.
15. Teng, M.W., Ngiow, S.F., von Scheidt, B., McLaughlin, N., Sparwasser, T., and Smyth, M.J. (2010). Conditional regulatory T-cell depletion releases adaptive immunity preventing carcinogenesis and suppressing established tumor growth. Cancer Res. *70*, 7800–7809.
16. Ziegler, S.F., and Buckner, J.H. (2006). Influence of FOXP3 on CD4+CD25+ regulatory T cells. Expert Rev. Clin. Immunol. *2*, 639–647.
17. Lu, L., Barbi, J., and Pan, F. (2017). The regulation of immune tolerance by FOXP3. Nat. Rev. Immunol. *17*, 703–717.
18. Zheng, Y., Josefowicz, S.Z., Kas, A., Chu, T.T., Gavin, M.A., and Rudensky, A.Y. (2007). Genome-wide analysis of Foxp3 target genes in developing and mature regulatory T cells. Nature *445*, 936–940.
19. Marson, A., Kretschmer, K., Frampton, G.M., Jacobsen, E.S., Polansky, J.K., MacIsaac, K.D., Levine, S.S., Fraenkel, E., von Boehmer, H., and Young, R.A. (2007). Foxp3 occupancy and regulation of key target genes during T-cell stimulation. Nature *445*, 931–935.
20. Samstein, R.M., Arvey, A., Josefowicz, S.Z., Peng, X., Reynolds, A., Sandstrom, R., Neph, S., Sabo, P., Kim, J.M., Liao, W., et al. (2012). Foxp3 exploits a pre-existent enhancer landscape for regulatory T cell lineage specification. Cell *151*, 153–166.
21. Polansky, J.K., Kretschmer, K., Freyer, J., Floess, S., Garbe, A., Baron, U., Olek, S., Hamann, A., von Boehmer, H., and Huehn, J. (2008). DNA methylation controls Foxp3 gene expression. Eur. J. Immunol. *38*, 1654–1663.
22. Zheng, Y., Josefowicz, S., Chaudhry, A., Peng, X.P., Forbush, K., and Rudensky, A.Y. (2010). Role of conserved non-coding DNA elements in the Foxp3 gene in regulatory T-cell fate. Nature *463*, 808–812.
23. Onizuka, S., Tawara, I., Shimizu, J., Sakaguchi, S., Fujita, T., and Nakayama, E. (1999). Tumor rejection by in vivo administration of anti-CD25 (interleukin-2 receptor alpha) monoclonal antibody. Cancer Res. *59*, 3128–3133.
24. Mattarollo, S.R., Steegh, K., Li, M., Duret, H., Foong Ngiow, S., and Smyth, M.J. (2013). Transient Foxp3(+) regulatory T-cell depletion enhances therapeutic anticancer vaccination targeting the immune-stimulatory properties of NKT cells. Immunol. Cell Biol. *91*, 105–114.
25. Foss, F.M. (2000). DAB(389)IL-2 (denileukin diftitox, ONTAK): a new fusion protein technology. Clin. Lymphoma *1* (*Suppl 1*), S27–S31.
26. Ghiringhelli, F., Menard, C., Puig, P.E., Ladoire, S., Roux, S., Martin, F., Solary, E., Le Cesne, A., Zitvogel, L., and Chauffert, B. (2007). Metronomic cyclophosphamide regimen selectively depletes CD4+CD25+ regulatory T cells and restores T and NK effector functions in end stage cancer patients. Cancer Immunol. Immunother. *56*, 641–648.
27. Morris, K.V., Chan, S.W., Jacobsen, S.E., and Looney, D.J. (2004). Small interfering RNA-induced transcriptional gene silencing in human cells. Science *305*, 1289–1292.
28. Castanotto, D., Tommasi, S., Li, M., Li, H., Yanow, S., Pfeifer, G.P., and Rossi, J.J. (2005). Short hairpin RNA-directed cytosine (CpG) methylation of the RASSF1A gene promoter in HeLa cells. Mol. Ther. *12*, 179–183.
29. Suzuki, K., Shijuuku, T., Fukamachi, T., Zaunders, J., Guillemin, G., Cooper, D., and Kelleher, A. (2005). Prolonged transcriptional silencing and CpG methylation induced by siRNAs targeted to the HIV-1 promoter region. J. RNAi Gene Silencing *1*, 66–78.
30. Zhou, J., Lazar, D., Li, H., Xia, X., Satheesan, S., Charlins, P., O'Mealy, D., Akkina, R., Saayman, S., Weinberg, M.S., et al. (2018). Receptor-targeted aptamer-siRNA conjugate-directed transcriptional regulation of HIV-1. Theranostics *8*, 1575–1590.
31. Berezhnoy, A., Brenneman, R., Bajgelman, M., Seales, D., and Gilboa, E. (2012). Thermal Stability of siRNA Modulates Aptamer- conjugated siRNA Inhibition. Mol. Ther. Nucleic Acids *1*, e51.
32. McNamara, J.O., Kolonias, D., Pastor, F., Mittler, R.S., Chen, L., Giangrande, P.H., Sullenger, B., and Gilboa, E. (2008). Multivalent 4-1BB binding aptamers costimulate CD8+ T cells and inhibit tumor growth in mice. J. Clin. Invest. *118*, 376–386.
33. Dranoff, G., Jaffee, E., Lazenby, A., Golumbek, P., Levitsky, H., Brose, K., Jackson, V., Hamada, H., Pardoll, D., and Mulligan, R.C. (1993). Vaccination with irradiated tumor cells engineered to secrete murine granulocyte-macrophage colony-stimulating factor stimulates potent, specific, and long-lasting anti-tumor immunity. Proc. Natl. Acad. Sci. USA *90*, 3539–3543.
34. Huehn, J., Polansky, J.K., and Hamann, A. (2009). Epigenetic control of FOXP3 expression: the key to a stable regulatory T-cell lineage? Nat. Rev. Immunol. *9*, 83–89.
35. Hawkins, P.G., Santoso, S., Adams, C., Anest, V., and Morris, K.V. (2009). Promoter targeted small RNAs induce long-term transcriptional gene silencing in human cells. Nucleic Acids Res. *37*, 2984–2995.
36. Manrique-Rincón, A.J., Beraldo, C.M., Toscaro, J.M., and Bajgelman, M.C. (2017). Exploring Synergy in Combinations of Tumor-Derived Vaccines That Harbor 4-1BBL, OX40L, and GM-CSF. Front. Immunol. *8*, 1150.
37. Tanaka, A., and Sakaguchi, S. (2019). Targeting Treg cells in cancer immunotherapy. Eur. J. Immunol. *49*, 1140–1146.
38. Magnuson, A.M., Kiner, E., Ergun, A., Park, J.S., Asinovski, N., Ortiz-Lopez, A., Kilcoyne, A., Paoluzzi-Tomada, E., Weissleder, R., Mathis, D., and Benoist, C. (2018). Identification and validation of a tumor-infiltrating Treg transcriptional signature conserved across species and tumor types. Proc. Natl. Acad. Sci. USA *115*, E10672–E10681.

39. Sharma, A., Subudhi, S.K., Blando, J., Scutti, J., Vence, L., Wargo, J., Allison, J.P., Ribas, A., and Sharma, P. (2019). Anti-CTLA-4 Immunotherapy Does Not Deplete FOXP3^{+} Regulatory T Cells (Tregs) in Human Cancers. Clin. Cancer Res. *25*, 1233–1238.

40. Turunen, M.P., Lehtola, T., Heinonen, S.E., Assefa, G.S., Korpisalo, P., Girnary, R., Glass, C.K., Väisänen, S., and Ylä-Herttuala, S. (2009). Efficient regulation of VEGF expression by promoter-targeted lentiviral shRNAs based on epigenetic mechanism: a novel example of epigenetherapy. Circ. Res. *105*, 604–609.

41. Suzuki, K., Hattori, S., Marks, K., Ahlenstiel, C., Maeda, Y., Ishida, T., Millington, M., Boyd, M., Symonds, G., Cooper, D.A., et al. (2013). Promoter Targeting shRNA Suppresses HIV-1 Infection In vivo Through Transcriptional Gene Silencing. Mol. Ther. Nucleic Acids *2*, e137.

42. Ackley, A., Lenox, A., Stapleton, K., Knowling, S., Lu, T., Sabir, K.S., Vogt, P.K., and Morris, K.V. (2013). An Algorithm for Generating Small RNAs Capable of Epigenetically Modulating Transcriptional Gene Silencing and Activation in Human Cells. Mol. Ther. Nucleic Acids *2*, e104.

43. Baron, U., Floess, S., Wieczorek, G., Baumann, K., Grützkau, A., Dong, J., Thiel, A., Boeld, T.J., Hoffmann, P., Edinger, M., et al. (2007). DNA demethylation in the human FOXP3 locus discriminates regulatory T cells from activated FOXP3(+) conventional T cells. Eur. J. Immunol. *37*, 2378–2389.

44. Josefowicz, S.Z., and Rudensky, A. (2009). Control of regulatory T cell lineage commitment and maintenance. Immunity *30*, 616–625.

45. Bailey-Bucktrout, S.L., and Bluestone, J.A. (2011). Regulatory T cells: stability revisited. Trends Immunol. *32*, 301–306.

46. Feng, Y., Arvey, A., Chinen, T., van der Veeken, J., Gasteiger, G., and Rudensky, A.Y. (2014). Control of the inheritance of regulatory T cell identity by a cis element in the Foxp3 locus. Cell *158*, 749–763.

47. Guo, J., and Zhou, X. (2015). Regulatory T cells turn pathogenic. Cell. Mol. Immunol. *12*, 525–532.

48. McNamara, J.O., 2nd, Andrechek, E.R., Wang, Y., Viles, K.D., Rempel, R.E., Gilboa, E., Sullenger, B.A., and Giangrande, P.H. (2006). Cell type-specific delivery of siRNAs with aptamer-siRNA chimeras. Nat. Biotechnol. *24*, 1005–1015.

49. Zhou, J., and Rossi, J. (2017). Aptamers as targeted therapeutics: current potential and challenges. Nat. Rev. Drug Discov. *16*, 440.

50. Pastor, F., Berraondo, P., Etxeberria, I., Frederick, J., Sahin, U., Gilboa, E., and Melero, I. (2018). An RNA toolbox for cancer immunotherapy. Nat. Rev. Drug Discov. *17*, 751–767.

51. Croft, M. (2003). Costimulation of T cells by OX40, 4-1BB, and CD27. Cytokine Growth Factor Rev. *14*, 265–273.

52. Arce Vargas, F., Furness, A.J.S., Solomon, I., Joshi, K., Mekkaoui, L., Lesko, M.H., Miranda Rota, E., Dahan, R., Georgiou, A., Sledzinska, A., et al.; Melanoma TRACERx Consortium; Renal TRACERx Consortium; Lung TRACERx Consortium (2017). Fc-Optimized Anti-CD25 Depletes Tumor-Infiltrating Regulatory T Cells and Synergizes with PD-1 Blockade to Eradicate Established Tumors. Immunity *46*, 577–586.

53. Quezada, S.A., Peggs, K.S., Curran, M.A., and Allison, J.P. (2006). CTLA4 blockade and GM-CSF combination immunotherapy alters the intratumor balance of effector and regulatory T cells. J. Clin. Invest. *116*, 1935–1945.

54. Loots, G.G., Ovcharenko, I., Pachter, L., Dubchak, I., and Rubin, E.M. (2002). rVista for comparative sequence-based discovery of functional transcription factor binding sites. Genome Res. *12*, 832–839.

55. Heale, B.S., Soifer, H.S., Bowers, C., and Rossi, J.J. (2005). siRNA target site secondary structure predictions using local stable substructures. Nucleic Acids Res. *33*, e30.

56. Kent, W.J. (2002). BLAT–the BLAST-like alignment tool. Genome Res. *12*, 656–664.

57. Strauss, B.E., Patrício, J.R., de Carvalho, A.C., and Bajgelman, M.C. (2006). A lentiviral vector with expression controlled by E2F-1: a potential tool for the study and treatment of proliferative diseases. Biochem. Biophys. Res. Commun. *348*, 1411–1418.

58. Reuter, J.S., and Mathews, D.H. (2010). RNAstructure: software for RNA secondary structure prediction and analysis. BMC Bioinformatics *11*, 129.

59. Rohde, C., Zhang, Y., Reinhardt, R., and Jeltsch, A. (2010). BISMA–fast and accurate bisulfite sequencing data analysis of individual clones from unique and repetitive sequences. BMC Bioinformatics *11*, 230.